

Microwave Properties of Borocarbide Superconductors $\text{LnNi}_2\text{B}_2\text{C}$ ($\text{Ln} = \text{Y}, \text{Er}, \text{Tm}, \text{Ho}$)

T. Jacobs, Balam A. Willemsen and S. Sridhar

Physics Department, Northeastern University, Boston, MA 02115,

R. Nagarajan, L. C. Gupta, Z. Hossain and Chandan Mazumdar

Tata Inst. of Fundamental Research, Colaba, Bombay, India,

P. C. Canfield and B. K. Cho

*Ames Laboratory and Dept. of Physics and Astronomy, Iowa State
University, Ames, IA.*

(November 19, 2018)

Abstract

We report measurements of the microwave surface impedance of the borocarbide family of superconductors $\text{LnNi}_2\text{B}_2\text{C}$ ($\text{Ln}=\text{Y}, \text{Er}, \text{Tm}, \text{Ho}$). The experiments enable direct measurements of the superfluid density, and are particularly sensitive to the influence of magnetic pairbreaking. In $\text{HoNi}_2\text{B}_2\text{C}$ the antiferromagnetic transition is clearly observed at zero field, and leads to a drastic reduction of the superfluid density, which recovers at lower temperatures. In $\text{ErNi}_2\text{B}_2\text{C}$ the antiferromagnetic transition is not seen in zero field data. Magnetic effects are responsible for anomalies in the low temperature surface impedance below approximately 4K in $\text{HoNi}_2\text{B}_2\text{C}$ and $\text{TmNi}_2\text{B}_2\text{C}$. The temperature dependence of the microwave impedance disagrees with simple BCS calculations.

Recently superconductivity was discovered in quaternary multiphase Y-Ni-B-C [1], in

multiphase Y-Pd-B-C system [2] and in single phase $\text{LnNi}_2\text{B}_2\text{C}$ ($\text{Ln}=\text{Y, Ho, Er, Tm, Lu}$) [3]. These materials are a class of intermetallic superconductors. While some members of the family, e.g. $\text{YNi}_2\text{B}_2\text{C}$, appear to show conventional superconducting behavior [4,5], other members, with $\text{Ln}=\text{Tm, Er, Ho}$, undergo an antiferromagnetic (AFM) transition at T_N , below the superconducting transition at T_c . Thus in addition to the important question of the nature of superconductivity issues concerning the interplay of magnetism and superconductivity arise in these materials.

Microwave measurements of superconductors yield unique information regarding the superfluid density, the quasiparticles and the nature of the pairing [6]. Despite the fact that magnetic superconductors such as ErRhB_4 have been known for about two decades, there have been few microwave studies of such superconductors. In this paper we report the first measurements of the microwave response of several members of the family, $\text{LnNi}_2\text{B}_2\text{C}$ with $\text{Ln} = \text{Y, Er, Tm, Ho}$.

Single crystals of $\text{LnNi}_2\text{B}_2\text{C}$ were grown out of Ni_2B flux. Details are provided in Ref. [5]. The crystals have a plate-like morphology and X-ray diffraction indicates that they have their crystallographic c-axis perpendicular to the surface of the plate. Powder X-ray diffraction on ground single crystals indicate that there is a small amount of Ni_2B flux contaminating the crystal, probably on the surface. This contamination is estimated to be below the 5% level. These crystals have been extensively characterized by a variety of techniques [5,7–9] besides the microwave studies discussed here. Polycrystalline samples of $\text{YNi}_2\text{B}_2\text{C}$ were also prepared and measured.

Microwave measurements were carried out in a Nb cavity using a high precision “hot finger” method [10], in which the cavity is maintained at 2 K while the sample temperature is varied from 2 K to as high as 200 K. The surface resistance of the sample is obtained from measurements of the resonator Q using $R_s = \Gamma [Q_s^{-1}(T) - Q_0^{-1}(T)]$, where Q_s and Q_0 are respectively the resonator Q’s with and without the sample. Similarly changes in the reactance are obtained from $\Delta X_s = \mu_0 \omega \Delta \lambda = (-2\Gamma/f_0) [f_s(T) - f_0(T)]$, where f_s and f_0 represent the resonant frequency with and without the sample. To get the absolute value

of the reactance, an indeterminate constant X_0 needs to be added. In materials which obey the skin depth limit in the normal state, one can use the criterion that $R_n = X_n$ above T_c to determine X_0 and so the absolute value of X_s . The geometric constant Γ was calculated, and confirmed using measurements on known samples of Cu. The method has been extensively validated via measurements on a variety of samples, from conventional low temperature superconductors, to high temperature superconducting crystals and films [11].

Because we are able to measure both the real and imaginary parts of the impedance $Z_s = R_s + iX_s$, it is possible to obtain the complex conductivity $\sigma_s = \sigma_1 - i\sigma_2$ from the present measurements, using the relation $Z_s = R_n \sqrt{2i/(\sigma_s/\sigma_n)}$, where R_n and σ_n are the normal state surface resistance and conductivity respectively. Of particular importance is the imaginary part σ_2 . This quantity is a measure of the superfluid density n_s which is proportional to σ_2 . It is also related to the penetration depth via $\sigma_2 = 1/\mu_0\omega\lambda^2$.

The microwave resistivity $\rho_{\mu n}(T)$ in the normal state, see Fig. 1, was obtained from the surface resistance using $R_n = \sqrt{\pi\mu_0 f \rho_{\mu n}}$ where μ_0 is the permeability of free space. The data is in good agreement with dc measurements [12], confirming that the classical skin-depth regime applies in the normal state.

YNi₂B₂C

The superconducting surface resistance $R_s(T)$ of several samples of YNi₂B₂C are shown in Fig. 2. The polycrystal shows higher R_n and also a slightly broader transition than single crystals. It is evident that R_s does not go to zero as $T \rightarrow 0$. Thus there is a residual surface resistance which is of the order of 10 – 20 mΩ and is, possibly, extrinsic in origin. This residual resistance does depend on sample characteristics such as crystallinity and surface preparation, being lowest for the polished single crystal #4. This is probably due to slight flux contamination which leads to a temperature-independent microwave loss.

Fig. 2 also shows the surface reactance $X_s(T)$. The absolute value was obtained by normalizing to $X_n = R_n$ above T_c . A striking feature of the reactance X_s data is the peak near T_c . This can be understood from simple models of the superconducting state such as two-fluid or BCS (see below). This is in fact occasionally observed in other superconductors, and

is due to buildup of superfluid, which leads to a situation where $\lambda > \delta_n$, the superconducting penetration depth is bigger than the normal state skin depth. This results in a peak in X_s which we have observed in $Y_1Ba_2Cu_3O_{1-\delta}$ [13] also. If we subtract the residual resistance from the low temperature reactance we can estimate a zero-temperature penetration depth $\lambda(0) = 1100\text{\AA}$ for sample #1. Although this method is not very sensitive to the absolute magnitudes the agreement with other estimates of $\lambda(0) = 1200\text{\AA}$ [5] is good.

TmNi₂B₂C

While the overall behavior of TmNi₂B₂C near and slightly below T_c is similar to the Y compound (see Fig. 3), a noteworthy feature is the *increase* of R_s at low temperatures. This is due to increasing magnetic coherence which results in a AFM transition at 1.5K [14], which is however just below the lower limit of our apparatus. This is also consistent with a decrease of H_{c2} observed in the same temperature region [15]. The data demonstrate that the microwave measurements can provide a measure of the magnetic scattering through the influence on the surface impedance of the superconducting state.

ErNi₂B₂C

The response of this compound appears similar to that of the Y compound as shown in Fig. 3. Interestingly the AFM transition which should occur at 6.0K [16,15] as observed in specific heat, dc-resistivity and magnetic susceptibility measurements, does not appear in the microwave data. Thus in this compound, the AFM transition is not accompanied by pairbreaking in zero field. There is however a weak shoulder in the R_s data at around 9.5 K which is not associated with a feature in any other measurement.

HoNi₂B₂C

A detailed plot of $R_s(T)$ vs. T in the region from 2K to 10K is shown in Fig. 4. The drop in R_s at the superconducting transition temperature of 8K is clearly seen. In all conventional superconductors, and in YNi₂B₂C as shown above, R_s decreases monotonically from the normal state value R_n . Remarkably, in HoNi₂B₂C R_s starts to increase again at around 6K. This is due to pair-breaking which accompanies the development of the antiferromagnetic state. At the AFM transition, R_s shows a *peak*. Peaks in R_s are never seen in conventional

superconductors, although non-monotonic dependence has been observed in $\text{Y}_1\text{Ba}_2\text{Cu}_3\text{O}_{1-\delta}$ [17].

It is very interesting to study the reactance as a function of temperature, also shown in Fig. 4. Below the superconducting transition at 8K , X_s increases due to the buildup of superfluid, as for the other superconductors, and then starts to decrease. However the AFM transition intervenes and appears as a peak, due to pairbreaking.

At low temperatures, both R_s and X_s are seen to *increase with decreasing T* . Although this is similar to that observed in $\text{TmNi}_2\text{B}_2\text{C}$, there is no AFM transition at a comparable temperature. Thus our data indicates a possibly new source of magnetic scattering below about 3.75K .

Complex Conductivity and Superfluid density

The real and imaginary parts of the conductivity σ_1 and σ_2 of $\text{YNi}_2\text{B}_2\text{C}$ are shown in Fig. 5. Note that a residual $R_{s,res}$ was subtracted while computing the complex conductivity. σ_2 has a “conventional” temperature dependence in that it rises smoothly at T_c to a large value at low temperatures. However the detailed temperature dependence does not fit any conventional form such as $(1 - t^4)$ of the 2-fluid model or a BCS form. Instead σ_2 appears to be well described by a $(1 - t)$ temperature dependence, except for a very slight curvature. σ_1 rises from its normal state value and has a peak at around $0.5T_c$. This is not the behavior expected from BCS coherence factors since there the peak is around $0.9T_c$. Instead this is similar to the behavior of σ_1 of $\text{YBa}_2\text{Cu}_3\text{O}_{7-\delta}$ where there is a peak at around $0.4T_c$ [17].

In $\text{HoNi}_2\text{B}_2\text{C}$, σ_2 and hence n_s are found to initially increase (see Fig. 5). However the AFM transition arrests this increase, and *reduces the superfluid density*, although superconductivity is not completely destroyed since σ_2 does not become zero. Below the AFM transition, σ_2 recovers. It is interesting that the behavior of σ_2 very closely mirrors that of H_{c2} [9]. The AFM transition is also reflected in the temperature dependence of σ_1 .

Discussion and Comparison with Theory

In order to address the issue of the nature of the superconducting order parameter, we plot the normalized surface resistance $(R_s(T) - R_{s,res})/R_s(T_c)$ vs. $t = T/T_c$ for all the

superconductors that were measured. The resulting plot shown in Fig. 6 is noteworthy in that the scaled plot appears to indicate a common, underlying temperature dependence, independent of sample, except of course for the expected deviations near T_N in $\text{HoNi}_2\text{B}_2\text{C}$ and the low temperature rise for $\text{HoNi}_2\text{B}_2\text{C}$ and $\text{TmNi}_2\text{B}_2\text{C}$. Also shown in Fig. 6 is a comparison with numerical calculations based on the BCS theory using a Mattis-Bardeen complex conductivity in the local limit [18]. The gap parameter $\Delta(0)/kT_c$ was used as an input parameter. The data do not agree with the numerical calculations if the mean-field value $\Delta(0)/kT_c = 1.74$ is used. Instead a much lower value 0.49 fits the data better. This appears to be in conflict with measurements which suggest a BCS s-wave state for the borocarbides. Indeed gap ratios of 1.45 to 1.95 for $\text{YNi}_2\text{B}_2\text{C}$ have been reported [14,19,20].

The data differ from the simple BCS analysis in three ways: (1) the broader temperature dependence which can be modeled as a smaller gap ratio, (2) the peaks at the AFM transition, and (3) the low temperature rise in $\text{HoNi}_2\text{B}_2\text{C}$ and $\text{TmNi}_2\text{B}_2\text{C}$. The latter two features can be attributed to pair-breaking by the magnetic constituents Ho and Tm. While the first feature could arise from sample inhomogeneities at the surface, an interesting question is whether the broadened transition could be due to an unidentified source of pairbreaking which should then be present in all the compounds. Equally noteworthy is the absence of any signature of the AFM transition in the *Er* superconductor. Neutron scattering studies of $\text{HoNi}_2\text{B}_2\text{C}$ [7] have shown the existence of a modulated magnetic structure from 6 K to about 4.7 K. Similar features are not observed in $\text{ErNi}_2\text{B}_2\text{C}$ [21,22]. Pairbreaking is significant only when there exists magnetic fields over length scales comparable to the coherence length, and this appears to occur in $\text{HoNi}_2\text{B}_2\text{C}$, but not in $\text{ErNi}_2\text{B}_2\text{C}$.

In conclusion, the microwave properties of several borocarbide superconductors reveal novel features of the superconducting state. The superfluid density which is obtained from the data displays striking features due to the influence of magnetic pairbreaking. The data reveal interesting results on the interplay of magnetism and superconductivity which deserve further experimental and theoretical studies.

Work at Northeastern was supported by NSF-DMR-9223850. Ames Laboratory is op-

erated for the U. S. Department of Energy by Iowa State University under Contract No. W-7405-Eng-82. Work at Ames was supported by the Director for Energy Research, Office of Basic Energy Sciences.

REFERENCES

- [1] R. Nagarajan *et al.*, Phys. Rev. Lett. **72**, 274 (1994).
- [2] R. J. Cava *et al.*, Nature **367**, 146 (1994).
- [3] R. J. Cava *et al.*, Nature **367**, 252 (1994).
- [4] S. A. Carter *et al.*, Phys. Rev. B **50**, 4216 (1994).
- [5] M. Xu *et al.*, Physica C **227**, 321 (1994).
- [6] S. Sridhar, D.-H. Wu, and W. L. Kennedy, Phys. Rev. Lett. **63**, 1873 (1989).
- [7] A. I. Goldman *et al.*, Phys. Rev. B **50**, 9668 (1994).
- [8] L. P. Le *et al.*, international Conference on Strongly Correlated Electron Systems, Amsterdam, The Netherlands, August 15-18, 1994 (unpublished).
- [9] P. C. Canfield *et al.*, Physica C **230**, 397 (1994).
- [10] S. Sridhar and W. L. Kennedy, Rev. Sci. Instrum. **59**, 531 (1988).
- [11] S. Oxx *et al.*, Physica C **235-240**, 889 (1994).
- [12] D. Naugle, private comm. (unpublished).
- [13] H. J. Chen, J. Owliaei, and S. Sridhar, Rev. Sci. Instrum. **65**, 2635 (1994).
- [14] R. Movshovich *et al.*, Physica C **227**, 381 (1994).
- [15] H. Eisaki *et al.*, Phys. Rev. B **50**, 647 (1994).
- [16] B. K. Cho, P. C. Canfield, L. L. Miller, and D. C. Johnston (unpublished).
- [17] D. A. Bonn, P. Dosanjh, R. Liang, and W. N. Hardy, Phys. Rev. Lett. **68**, 2390 (1992).
- [18] D. C. Mattis and J. Bardeen, Phys. Rev. **111**, 412 (1958).
- [19] T. Ekino *et al.*, Physica C **235-240**, 2529 (1994).

[20] T. Hasegawa *et al.*, *Physica C* **235-240**, 1859 (1994).

[21] S. K. Sinha *et al.*, *Phys. Rev. B* **51**, 681 (1995).

[22] J. Zarestky *et al.*, *Phys. Rev. B* **51**, 678 (1994).

FIGURES

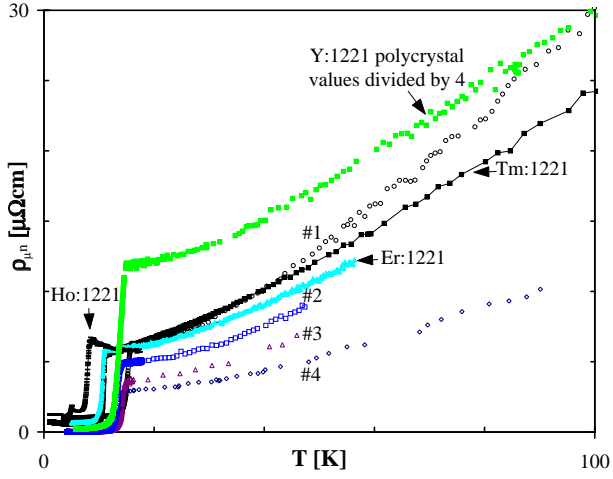


FIG. 1. Microwave resistivity of LnNi_2B_2 ($\text{Ln}=\text{Y}, \text{Er}, \text{Tm}, \text{Ho}$) in the normal and superconducting states extracted from the surface resistance. #1 to #4 are different $\text{YNi}_2\text{B}_2\text{C}$ single crystal samples.

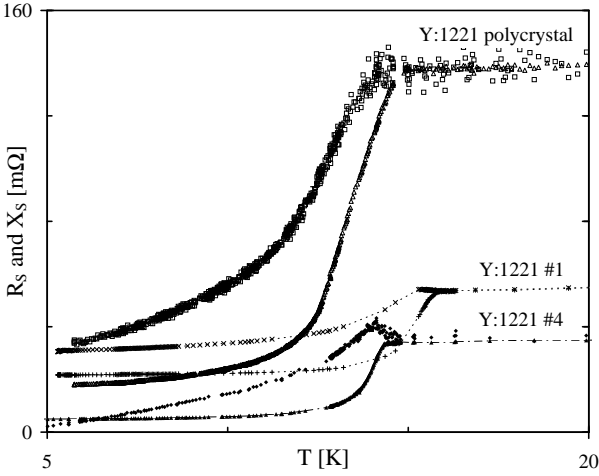


FIG. 2. R_s and X_s of $\text{YNi}_2\text{B}_2\text{C}$ in the superconducting state for a polycrystal and single crystals (#1 and #4).

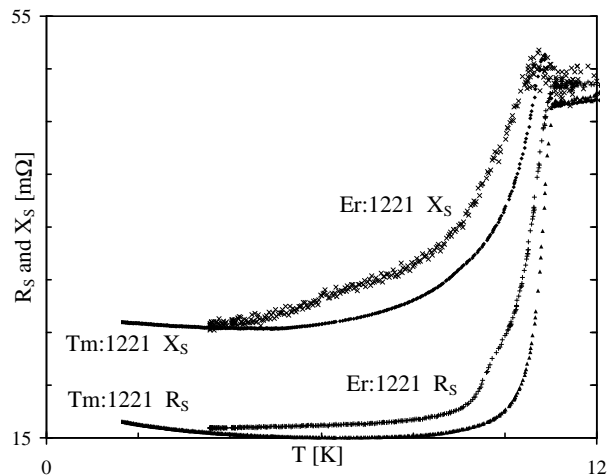


FIG. 3. R_s and X_s of $\text{TmNi}_2\text{B}_2\text{C}$ and $\text{ErNi}_2\text{B}_2\text{C}$.

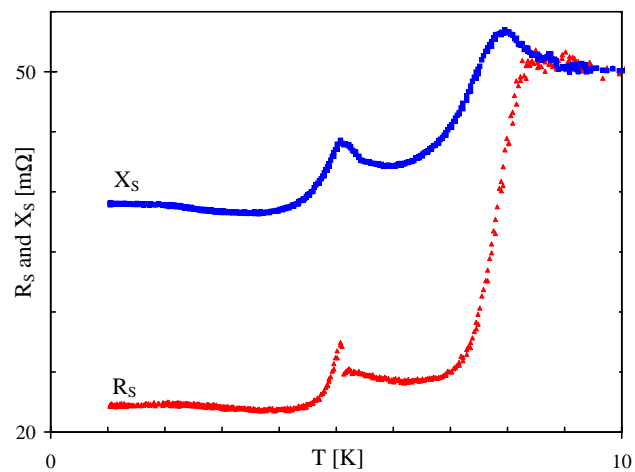


FIG. 4. R_s and X_s of $\text{HoNi}_2\text{B}_2\text{C}$. The AFM transition at 5.2 K is clearly visible.

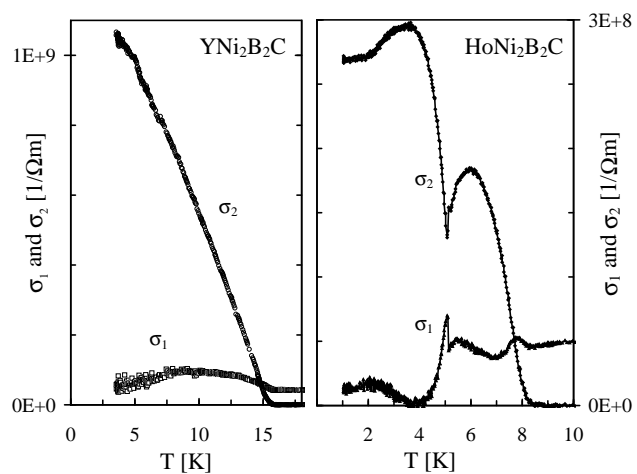


FIG. 5. Real (σ_1) and imaginary (σ_2) parts of the complex conductivity of (left) $\text{YNi}_2\text{B}_2\text{C}$ and (right) unpolished $\text{HoNi}_2\text{B}_2\text{C}$ sample. σ_2 is proportional to the superfluid pair density.

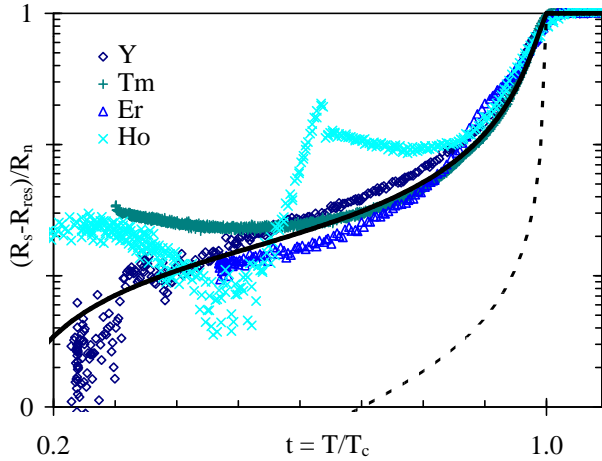


FIG. 6. Normalised surface resistance of $\text{LnNi}_2\text{B}_2\text{C}$ ($\text{Ln} = \text{Y}, \text{Tm}, \text{Er}, \text{Ho}$) in the superconducting states vs. reduced temperature. The residual $R_s(T \rightarrow 0)$ has been subtracted out in each case. Also shown are BCS calculations with $\Delta(0)/kT_c = 1.74$ (dashed line) and 0.45 (solid line).